Finite Element Analysis of Thin Disk in Fortran

B. Himberg

Abstract

Finite Element Methods are ubiquitous in Materials Science. They represent the melding of boundary conditions and partial differential equations. Here such a method combines a fourth order partial differential equation in polar coordinates with a simply supported circular plate. Focusing on the maximum deflection, a comparison of of this finite element method is made to the analytic results for a steel plate under uniform pressure. The primary contribution to error is found to be the ratio of plate thickness to plate support length, proportional to the radius here.

Keywords: Finite Element Method, Finite Element Analysis, Thin Plate

1. Introduction

Typically analytic solutions are limited to simpler conditions, however these solutions can be used to validate numerical methods. Once benchmarked, such numerical methods can then be used to evaluate properties of much more complex problems. This paper presents a comparison of the Finite Element Method to an analytic solution with a focus on sources of error due to support length ratio and pressure, material specifics such as Young's Modulus or Poisson's Ratio, and finally tunable parameters such as the number of finite elements.

The benchmark used here is the maximum deflection of a simply supported circular thin plate under uniform pressure. Simply supported means that the edges are fixed: any node on the edge is constrained to remain stationary. Intuition suggests that the plate will have greater deflection away from the edges, leading to maximum deflection at the center of the plate.

The analytic solution and finite element method share the same differential equation, to be found in [1, 2]. High level details are presented in section 2 before the finite element method used here, a Fortran implementation [3] which this author has modified for extended capabilities, is discussed in section 3. Graphical results can be found in section 4, followed by a discussion of future work in section 5.

Finally note that all the data, and the code used to obtain it, can be found on GitHub [4] as well as the source code and graphs for this paper.

2. Analytic Method

Both the analytic solution and finite element method begin with the same differential equation

$$\nabla^2\nabla^2 w = \frac{P}{D} \tag{1}$$

where P is the pressure and D is the flexural rigidity. This is the most general form, and is

also a starting point for square plates.

The Laplacian operator is often involved in finite element methods. Here we use its polar coordinates definition to arrive at

$$\nabla^2\nabla^2 w = \left(\frac{\partial^2}{\partial r^2} + \frac{1}{r}\frac{\partial}{\partial r} + \frac{1}{r^2}\frac{\partial^2}{\partial \theta^2}\right)\left(\frac{\partial^2 w}{\partial r^2} + \frac{1}{r}\frac{\partial w}{\partial r} + \frac{1}{r^2}\frac{\partial^2 w}{\partial \theta^2}\right) = \frac{P}{D} \tag{2}$$

which may be simplified by supporting the plate symmetrically with respect to the z-axis. This eliminates the θ dependency of eq. (2), leading to

$$\left(\frac{\partial^2}{\partial r^2} + \frac{1}{r}\frac{\partial}{\partial r}\right)\left(\frac{\partial^2 w}{\partial r^2} + \frac{1}{r}\frac{\partial w}{\partial r}\right) = \frac{P}{D} \tag{3}$$

for which the solution

$$w(r) = \frac{Pr^4}{64D} + A_1 + B_1 r^2 \tag{4}$$

exists. The case of simply supported edges can be shown [2] to yield

$$w(r) = \frac{Pa^4}{64D}\left[1 - \left(\frac{r}{a}\right)^2\right]\left[\frac{5+\nu}{1+\nu} - \left(\frac{r}{a}\right)^2\right] \tag{5}$$

which presents the new variables a, the radius of the disk, and Poisson's Ratio ν. Here r is the point at which deflection is measured and, happening to be the origin, simplifies the equation even further. First though, flexural rigidity may be defined as

$$D = \frac{E^2 h^3}{12(1-\nu^2)} \tag{6}$$

which is applied to eq. (5) to arrive the final expression

$$w_{max}(a) = \frac{3Pa^4}{16Eh^3}(5+\nu)(1-\nu) \tag{7}$$

for w_{max}, the maximum deflection at the center of a disc under uniform constant pressure p. Here E and ν are Young's Modulus and Poisson's ratio, properties of the material the disc is comprised of. The height h and radius r are measurements of the spatial extent of the disc, and their ratio must be i$h/r < 0.1$ in order to match with experimental results [2].

3. Finite Element Method

Finite element methods (FEMs) have a very specific set of requirements: boundary conditions, on an equation describing the interaction of adjacent domains. They are not unlike projection methods used in quantum Monte Carlo (QMC). For example in the case of Path Integral Ground State (PIGS) [5] one would use a known wavefunction at two boundaries in imaginary time and propagate them towards the center using the unitary time operator. The PIGS case warrants mentioning because it satisfies this specific set of conditions: it has a well defined boundary and a differential equation (the Hamiltonian, second order) describing how domains, which could be the position of particles or even a particle count using second quantization, interact.

Domains interact via eq. (3) in the case of deflection of a disk . While in PIGS domains are points, here domains are finite elements: specifically they are triangular and have an area. They may move up or down on the z-axis and may also rotate in two orthogonal directions (for example about the x-axis and y-axis). The boundary is fixed on the z-axis:

nodes, the corners of a finite element, which reside on the edge may not move up or down. They may however rotate. Consider fig. 1 where only half the plate is rendered since,

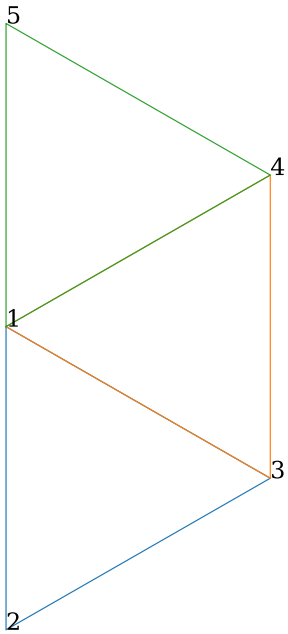

Figure 1: This mesh has three finite elements and five nodes. The nature of FEM is that a domain is split into smaller domains which interact with each other at the boundaries. The center node will always be designated as the first node and is the node where deflection is measured.

with the proper boundary conditions, only half the plate is necessary to run the FEM. There are three finite elements in this figure, each being a triangle. Each triangle, or (finite) element has three corners, or nodes. All elements share at least 2 nodes with other elements. This is important since this connection is what allows the boundary conditions at the edge to propagate to center. Note that there are currently more nodes (5) than elements (3). Another ring may be added as in fig. 2 and now there are an equal number of nodes and elements (10). Note also that while in fig. 1 the area of each element is clearly equal, this is not the case for fig. 2.

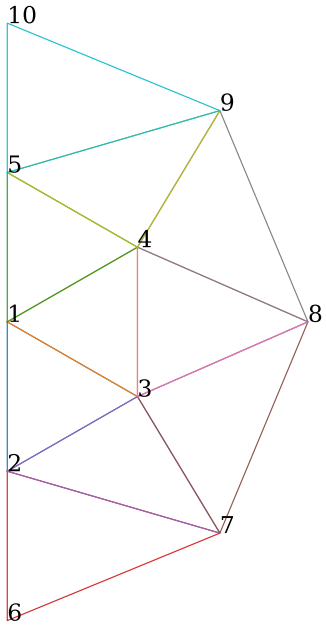

Figure 2: This mesh has ten finite elements and ten nodes. The number of elements is related to the number of nodes on a ring as $\sum_{i=4}^{5}(2 * i - 1)$ in this case since there are two rings: the innermost ring with 4 nodes and the outermost with 5 nodes. The number of nodes will always be lesser than the number of elements past this point.

A significant amount of time went into programming an algorithm to generate meshes of arbitrary size, as well as automating the production of these plots. For all the runs to follow, with the exception of the finite element count scaling run, a mesh with 898 elements as in fig. 3 was used. While none of the meshes have finite elements with precisely the same area, which is important since the area determines the amount of pressure a single finite element feels and therefor affects its relative contribution to the mesh, as the number of elements scales up the standard deviation goes down: we approach the continuum limit. For the mesh in fig. 3, the average area is $109.13(2)\,\mathrm{mm}^2$.

Finally it warrants discussing the expansion of the Fortran code mentioned earlier:

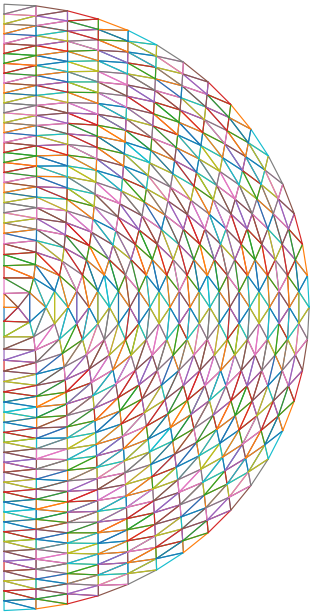

Figure 3: This mesh has 898 finite elements and 494 nodes, and was used for the majority of the results in section 4. The elements near center are concerning since they have more area than those near the edge, and in general the area appears irregular about center. There is also an open question as to whether the general orientation of finite elements is important.

P	$1.4072\,\mathrm{Nmm}^{-2}$
E	$20\,394\,\mathrm{Nmm}^{-2}$
a	$250.00\,\mathrm{mm}$
h	$25.000\,\mathrm{mm}$
ν	0.29000

Table 1: These are the parameters used for all graphs to follow. Each graph will treat a parameter as tunable while locking the others: the idea is to test a range of values. The material used here is steel, and is an elastically isotropic material.

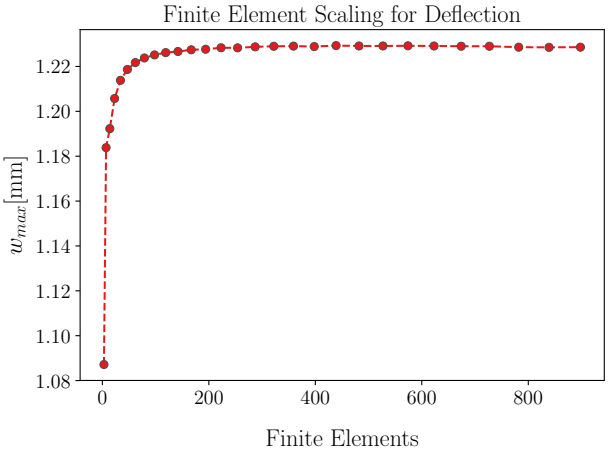

Figure 4: The density of points is lower on this plot than those to follow because of the mesh generation method chosen: not all possible configurations between 4 and 898 nodes were generated. Parameters used are precisely those used in table 1, with the minimum number of elements 3 and the maximum 898.

the original code was only capable of handling 170 elements. The code was successfully modified to handle up to 900 elements for this paper.

4. Comparison

For this entire section a set of constant were chosen from [2], problem 13.16. Each graph to follow with keep all but one parameter constant, which will be noted. Consider table 1 where the variables correspond to the pressure, Young's modulus, radius, thickness, and Poisson's ratio respectively. Unless stated otherwise, the mesh will be as in fig. 3 with 898 elements and 494 nodes.

Figure 4 considers only the actual deflection as a function of the number of elements used by the finite element method. There is clearly an asymptotic behavior present, which seems reasonable since as the number of elements increases their effective area decreases and we are approaching the continuum limit (that is, moving to the non-finite element realm) where the actual, exact, solution exists. Consider table 2 for a comparison to the expected value. It seems that FEM values are reasonably close: within 1.2 percent. This is encouraging, and so next potential sources of error are examined by allowing a single parameter to vary, each in turn, while locking the remaining parameters. Ideally the following plots will either appear

FEM	1.2285 mm
ANA	1.2147 mm

Table 2: This is a comparison of the final point in fig. 4 and the expected value from eq. (7). The error is within 1.2 percent. Parameters used are precisely those used in table 1.

random, with a small variance, or even better flat.

Consider fig. 5 where pressure is treated as

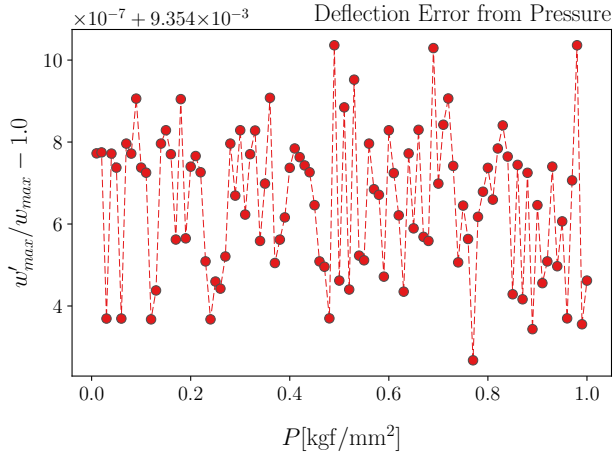

Figure 5: This is another plot of the relative error between the finite element method and the analytic method. Note the top left corner: these values are all within 0.9 percent error. The parameters used here are as in table 1, except that the pressure P varies. The mesh in fig. 3 was used for all points in all graphs to follow.

the tunable parameter. Pressure can have a dramatic effect on the system, being directly related to deflection since it is in a sense the cause of deflection. It appears however that pressure has little effect on the error: this looks like noise, and is likely related to the inconsistency of element area in the generated mesh. Yet taking a second look, note the magnitude of the error: it is constant, around 0.9 percent. The errors are too large to be rounding errors. It may be related to the underlying algorithm of the 'Plates' FEM, specifically the order of the method used to approximate the ∇^2.

Next consider what happens when the ratio between thickness h and r, the radius, becomes the tunable parameter. The expectation is that as this ratio approaches 1.0, the error will increase. Unfortunately both the analytic method and finite element method are derived from the same principles and the error noted here is relative error between the two: it should be thought of as a measure of the FEM method as a replacement of the analytic method, not a measure of how correct either method in the thick plate regime. Figure 6 shows that the two

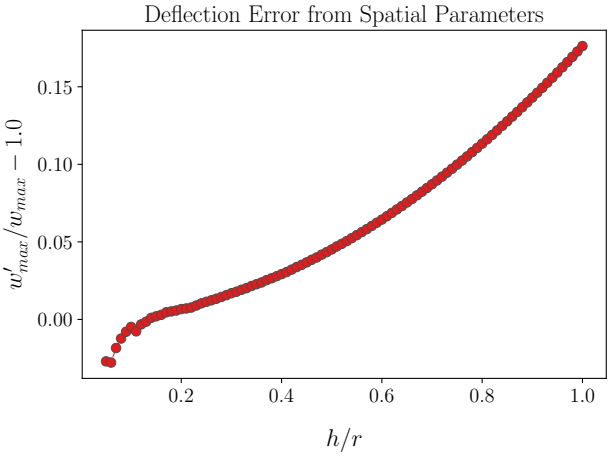

Figure 6: The relative error between the FEM and analytic data. There seems to be a strong divergence here as the thickness increases, the ratio of h/r approaching unity. While this divergence favors the finite element method, in reality the two should agree with respect to thickness. It could be related to the elements in the center of fig. 3 being notably larger than all other elements.

methods diverge. This divergence is in favor of the FEM method. Experiments have shown that as thickness increases, the calculated deflection is much less than the measured and in fact a prefactor

$$C = 1 + 5.72\left(\frac{h}{a}\right)^2 \tag{8}$$

is necessary, with a as the radius to match eq. (7).

Now a look at the material parameters, Young's modulus and Poisson's ratio, remains. Considering eq. (7), Young's modulus E is of the same order as the pressure P. This suggests any errors should also be on the same order, specifically varying E isn't expected to cause the two methods to diverge. Figure 7 supports

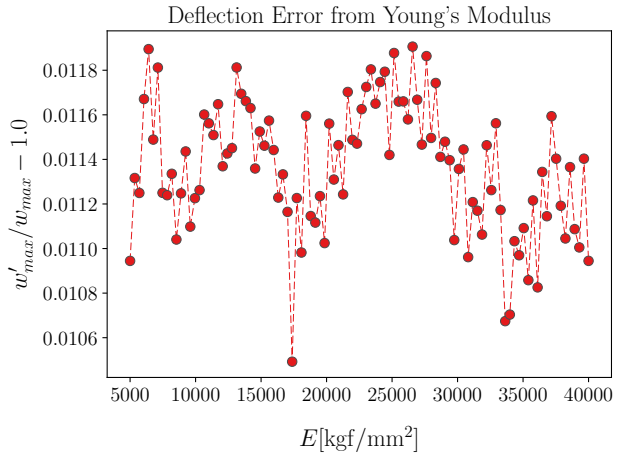

Figure 7: The error here seems to be systematic: it appears constant, with some small variation about the average. At least for this range, error won't increase or decrease with changes to Young's modulus.

this expectation with what seems a constant error, however the magnitude is within 1.2 percent, slightly larger than the 0.9 percent found with pressure.

Finally a look at ν which has a more complicated relationship with w_{max}: it scales quadratically. The result is as in fig. 8 where divergence between the finite element method and the analytic solution increases as a function of ν, though being a ratio within the range presented for most materials and the maximum error here being below 1.5 percent makes it less of an issue.

5. Discussion

The results presented indicate that for thin plates, where the plate thickness is a tenth or

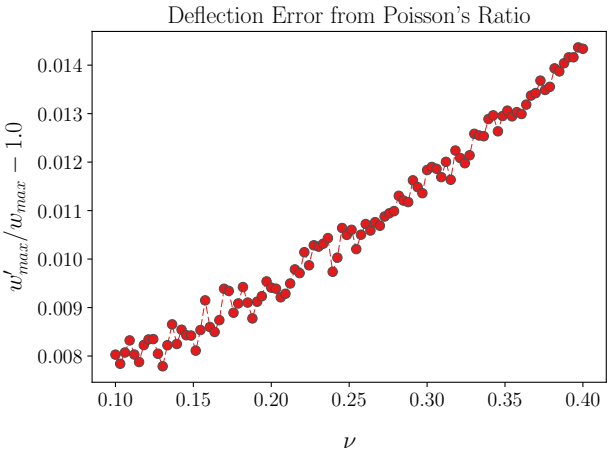

Figure 8: Since ν is a ratio, the range presented here is reasonable. There certainly is some scaling present with respect. The error though is within 1.5 percent.

less of the plates radius, the FEM method certainly matches the analytic method. The error seems independent of Young's modulus and pressure. Error increases as poison's ratio increases, however for most materials the error is small. That leaves the error due to the ratio of plate thickness and plate radius.

For the parameters in table 1 the magnitude of the deflection increased as the ratio approached 1.0. This is in agreement with experimental expectations, and may be justifiable to an extent: domains have finite size and materials have structure, impurities. The analytic solution treats the material as pure and continuous. Still, while the FEM method is technically closer in this regime, it is not near close enough. A ratio of 1.0 should correspond to a prefactor of 6.72 in eq. (8), yet the FEM 'prefactor' is only 1.15.

Overall this FEM is intended to solve more difficult problems which still fall in the thin plate regime, such as non-uniform thickness or a varying pressure across the surface or perhaps holes which are not aligned to origin. Future work would involve improving mesh generation, and perhaps implementing a higher or-

der Laplacian operator to decrease error. Finally, this method may lend itself well to GPU computation.

[1] O. Zienkiewicz, The finite element method in engineering science, McGraw-Hill, 1971.
URL https://books.google.com/books?id=_d1RAAAAMAAJ

[2] A. Boresi, R. Schmidt, Advanced mechanics of materials, John Wiley & Sons, 2003.
URL https://books.google.com/books?id=eLMeAQAAIAAJ

[3] T. Taki, Plates, http://www.geocities.jp/toshimi_taki/plate/plate.htm (2004).

[4] B. E. Himberg, Plates, https://github.com/bhimberg/plates (2017).

[5] A. Sarsa, K. E. Schmidt, W. R. Magro, A path integral ground state method, The Journal of Chemical Physics 113 (4) (2000) 1366–1371. arXiv:http://dx.doi.org/10.1063/1.481926, doi:10.1063/1.481926.
URL http://dx.doi.org/10.1063/1.481926